



THERMAL EFFICIENCY MEASUREMENT DURING ATIG AND TIG WELDING

Thiago José Donegá

Universidade Federal do Triângulo Mineiro, Randolfo Borges Junior, 1250, Univerdecidade, Uberaba - MG
donega.uftm@yahoo.com.br

Thonson Ferreira Costa

Universidade Federal de Uberlândia, João Naves de Ávila, 2121, Santa Mônica, Uberlândia - MG
thonsoncosta@yahoo.com.br

Louriel Oliveira Vilarinho

Universidade Federal de Uberlândia, João Naves de Ávila, 2121, Santa Mônica, Uberlândia - MG
vilarinho@mecanica.ufu.br

Abstract. *The ATIG process (TIG welding with active flux) consists in depositing a thin layer of flux on the workpiece surface just before the welding. The layer deposition can be done by brushing or spraying over the surface, and welding is performed after it dries out. It is found that with this process it is possible to increase productivity (travel speed) up to three times higher compared to the conventional TIG process. However, the physical phenomena associated with this practical gain of productivity still remains under discussion. Thus, the aim of this paper is to analyze the thermal efficiency and heat input in the welding process with the ATIG compared with conventional TIG process, using liquid-nitrogen calorimeter, as a contribution to better understanding the physical associated phenomena. Autogenous welding was performed automatically directly on plate AISI 304 austenitic stainless steel. At the end of welding, the test plate is brought automatically into the recipient (dewar) containing liquid nitrogen. Dedicated monitoring was performed by data acquisition of voltage and current signals. As well as the mass variation signal from a digital balance, which is under the dewar. After welding, geometrical parameters of the weld bead were measured by profile projector. In accordance with previous studies, it is concluded that the weld penetration during ATIG process is deeper than the one achieved by conventional TIG welding. In addition, it is possible to conclude that the thermal efficiency of the ATIG welding is lower than the efficiency in conventional TIG welding. Thus, there are two main effects, which have different trends. The first is the effect of arc constriction, which tends to increase the current density observed in the smaller bead width. The second effect is the lower thermal efficiency, which leads to lower heat input, thus reducing penetration. From the presented results, the effect of the arc constriction is more pronounced than the reduction of efficiency.*

Keywords: ATIG, Flux, Thermal Efficiency

1. INTRODUCTION

Developed in the 60s by Paton Welding Institute, the process ATIG (TIG welding with active flux), consists in depositing a thin layer of flux on the workpiece surface just before the welding. According to Azevedo (2009), the flux is a solution formed by oxides or fluorides mixed with a solvent, that can be acetone, alcohol or water. The layer deposition can be done by brushing or spraying over the surface and welding is performed after it dries out. It is found that with this process it is possible to increase productivity (travel speed) up to three times higher compared to the conventional TIG process (Azevedo, 2009; Anderson and Wiktorowicz, 1996).

Kumar (2009) highlights that, although is a single process, that is enough to apply a flux on the workpiece surface just before the welding, the physical phenomena associated with the penetration increase of the ATIG weld still remains under discussion. Between studies approached to seek explanations about the responsible mechanisms for the increased penetration ATIG weld, can cite Modenesi (1999), that evaluated fluxes with different compositions to try justify the use of one or other flux. This author showed that the use of flux in the TIG weld, even if the single formulation (single-component fluxes), can increase the welding penetration efficiently. Vilarinho (2010a) used a mixture based flux silicate which provided increase weld penetration to be applied in a wide range of materials, including austenitic stainless steel.

Aiming to understand the behavior of the heat flux and the temperature difference when comparing the thermal cycles obtained during the welding ATIG and TIG conventional, Vilarinho (2010b) concluded that temperatures on the ATIG process are greater and the heat flux to the TIG process have bidimensional characteristics while in the ATIG process they are three-dimensional so that have big flux component of heat on the thickness direction that can contribute to the penetration increase.

On the other hand, is not found in the literature about the thermal efficiency of the ATIG process, in other words, studies that contributed quantify the heat input on the workpiece during the ATIG welding. Considering that the heat

input is a parameter that influences decisively on the welding process, both industrially and in research, due to its direct link with changes in metallurgical characteristics and mechanical properties of the welded joint (Vilarinho, 2010b), is important to check wich paper of the flux (of the ATIG process) in the heat input of the process.

Thus, the aim of this paper is to analyze the thermal efficiency and heat input in the welding process with the ATIG compared with conventional TIG process, using liquid-nitrogen calorimeter, as a contribution to better understanding the associated physical phenomena.

2. MATERIALS AND METHODS

2.1 Aplication of the active flux

To carry out the welding ATIG, was applied manually a flux-based silicate salts using a external mixing airbrush (air and flux mixed outside of the airbrush), the compressed air pressure was adjust in three bars, the application was done with two passed of the flux jet on each workpiece from one side to another in the direction of welding, obtaining at the end a uniform medium layer of $39 \pm 7 \mu\text{m}$, wich was measure by a digital layer measurer Mitutoyo Digi-Derm with resolution $\pm 3 \mu\text{m}$ and nominal range from 0 to 1 mm. The thickness of layer was obtained measuring the layer in three points (extremities an middle of the workpiece) and later was calculate the mean and standard deviation of these measure. The application distance from the airbrush nozzle to workpiece was 100 mm, and the dry time of the flux between the application and measure of the thickness layer was 10 minutes.

2.2 Welding

In all welding used plates austenitic stainless steel AISI 304, dimensions 165 x 51 x 4 mm. The gas shielding flow was 12 l/min, tungsten electrode AWS WTh-2 diameter 2.4 mm, the vertex angle of electrode was 60° , and its posicioned 10 mm outside the nozzle, the diameter nozzle was 8 mm. The welding current (I), travel speed (Vs), gas shielding, workpiece with flux (ATIG) and without flux (TIG), the distance from the electrode to workpiece (DEP) were varied to each test realized, and are shown on the Tab. 1.

Table 1. Parameters varied in each test.

Test	Process	Gas shielding	I (A)	Vs (cm/min)	I/Vs (Amin/cm)	DEP (mm)
1A	A-TIG	Ar Pure	100	15	7.0	2.0
2A						3.0
3A			150	27	6.0	2.0
4A						3.0
5A		Ar+25%He	100	15	7.0	2.0
6A						3.0
7A			150	27	6.0	2.0
8A						3.0
1T	TIG	Ar Pure	100	15	7.0	2.0
2T						3.0
3T			150	27	6.0	2.0
4T						3.0
5T		Ar+25%He	100	15	7.0	2.0
6T						3.0
7T			150	27	6.0	2.0
8T						3.0

Beginning the test plates would be welded using two current values and one travel speed (Vs). But, during the preliminary tests it verifies that the workpieces were having “drilling” with the current of 150 A together the travel speed 15.0 cm/min. The alternative find to solve this problem was decrease the welding power (E) to these tests. To calculate the welding power (Eq. 1), are necessary the tension value (V), current (I) and travel speed (Vs). From this adjust were generate two relations of I/Vs to obtain values of the E near. Therefore, from this relation was obtained two values for the I/Vs that are 6.0 Amin/cm and 7.0 Amin/cm.

$$E = \frac{P_{inst}}{V_s} \quad (1)$$

The welding were done in a automatized table of the liquid-nitrogen (N_2L) calorimeter, that is used to quantificate the power absorbed by the plate on a welding process. For both the equipment have an automatic system to movement the torch with limit that is actioned in the end of the weld and make the claw, that is catching the workpiece, to discharge it slowly on the dewar recipient (similar to the coffee bottle with large mouth) containing N_2L . This recipient was on a digital balance with signal out and an acquisition basis system to register the mass loss by the evaporation of the N_2L due to the entrance hot workpiece, on the dewar, because the welding process (Arevalo, 2012). During the welding are registered the electrical signals of tension (U_i) and current (I_i) of the welding source to calculate the mean instantaneous power (P_{inst}) of the electrical arc, according to the Eq. (2) to a datum number n of points. The relation between potency and travel speed gives origin to the power weld, most commonly used in the welding technique, albeit erroneous (the correct is heat input). The acquisition system of the electrical signals tension and current of the welding source, beyond the balance signal, consists to a plate of dedicate signal conditioning (Arevalo, 2012), wich processes the signals to be processed by the acquisition plate NI USB 6215 with data acquisition rate of 2000 Hz.

$$P_{inst} = (\sum_{i=1}^n (U_i * I_i)) / n \quad (2)$$

From the measurement to the evaporated mass of N_2L is possible to estimate the heat wich was in the workpiece when it was put on the dewar recipient, and that causes nitrogen evaporation. Therefore assumes the heat plate is fully converted to latent heat of vaporization of N_2L . Once known the evaporated mass of the nitrogen and it latent heat (198.6 J/g) (Arevalo, 2012), estimated heat input of the workpiece. However, needed to observe that this heat is relacioned to the temperature variation between the welding temperature and the N_2L temperature (-195.8 °C), wich is not the welding reality, because the thermal flux of the process referred the cooling of the workpiece from the temperature during the welding to environment temperature. Thus, after the welding and remove the workpiece from the dewar recipient, needed to await that the workpiece arrive the environment temperature again, and reinsert it over again in the dewar recipient, to calculate the heat relative to the cooling from environment temperature to N_2L temperature. By subtracting both measures, haved the heat input of the process relacioned to the cooling of the temperature during the welding to the environment temperature.

On this methodology needed to attempt the environment temperature variations and the humidity, to effectuate correlations in the evaporate mass of the N_2L , beyond to discount the mass of the workpiece more the bead mass. More details are presented in the reference (Arevalo, 2012). More specifically to this paper, when the workpiece is immerse on the N_2L into the recipient dewar, is necessary to adjust the acquisition time to guarantee that the data register was done from the moment of the immersion to stabilization of the evaporation (thermal equilibrium between the N_2L and the workpiece). In this sense, the acquisition data time of the balance to the workpiece with the welding heat was adjust in 200 seconds, and the time to the workpieces in the environment temperature was 180 seconds, in conformity with preceding tests (Arevalo, 2011).

At the end knowing the heat input in the workpiece per unit length of the bead weld and the welding power, estimated the thermal efficiency by the relation of these.

2.3 Inlay and geometric analisys

Due to the low temperature at wich underwent the workpiece when were immersed on the N_2L , new workpieces were welding using the same parameters of the Tab. 1, to be used to the measure of the geometric parameters of the weld bead, in other words, without the realization of this temper in the N_2L . These new workpiece were prepared according to Fig. 1, in other words, it applied the ATIG flux only in one half surface of the workpiece, according to the practice of other authors (Azevedo, 2009). Be detached that the feeling of the welding is from the one half without flux to the one half with flux, so don't have possible to have contamination of the arc weld by the flux, if have had done on contrary.

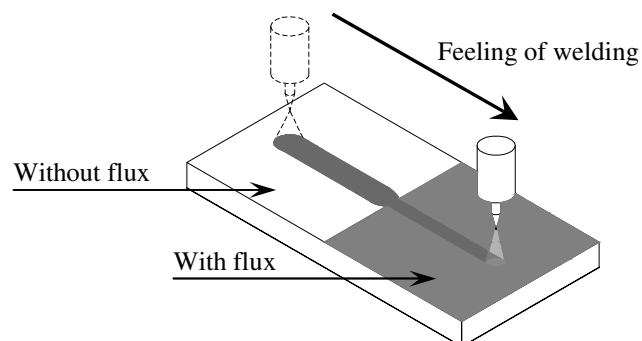


Figure 1. Schema of the flux workpiece welded to the geometric analysis.

After the weldings, the workpieces were cut transversally, from where take one sample done by the ATIG process and other done by the TIG welding, both with 10 x 20 mm. It is noteworthy that at the area with the weld change from the region without flux to the region with flux were reject 10 mm on each side, so that to avoid instability region. After cutted, Inlayed the samples by form that in each inlay put one ATIG weld sample and one TIG weld sample, refers the same workpiece.

The inlay sample were manually sanding using sandpaper water on granulometry 180, 220, 320, 400, 600 e 1200. After each sandpaper the sample was rotated 90° and was sanded until the previous sanding signals disappearing. The chemical attach to show the weld profile was done with the Marble reagent.

2.4 Measurement of the linear parameters

To determinate the bead weld geometry, used the dimensions present in the Fig. 2, wich are show the linear parameters of the welding bead.

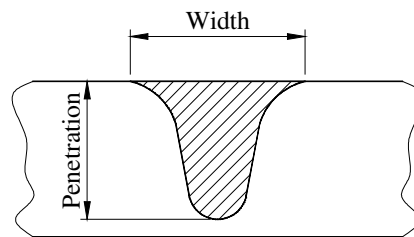


Figure 2. Illustration of the dimensions taken on the measure of the bead welding.

The measurement of the linear parameter was done using a digital Profile Projector manufacture by Mitutoyo model PJA3000, with resolution to linear measurement of 0.001 mm and nominal rate of 50 mm to the axis X and Y. During the measurement was used an amplification lens of 10X.

3. RESULTS AND DISCUSSION

From the methodology described on Item 2, the Tab. 2 gives the results of the thermal efficiency (Nt) obtained on each test to the ATIG and TIG process. The results obtained to the thermal efficiency to the TIG process without flux, presented in the Tab. 2, are according to that find on literature (Arevalo, 2012; Dupont and Marder, 1995; Fuershbach, 1991), wich present values between 61% to 79% of thermal efficiency, according to the welding conditions. Thus, can be assert that the achieved values to the thermal efficiency to the TIG process without flux are according to the other authors.

To a better understanding of the factor effects on the thermal efficiency, it was decided to realize the variance analysis (ANOVA) about the obtained results, shown on the Tab. 3. Altogether, by means of this table, observed that the level of significance “p” is more expressive to the effect of I/Vs. This means that the I/Vs is the factor that influenced more on the thermal efficiency. Other factor that also have a significance level “p” considerable was the DEP. By this analysis it is possible to note that the variation on the parameter of these two variable presents is which cause more influence on the thermal efficiency results. On this context, which is observed is that the significance on the use of different processes (ATIG ou TIG) do not influences significantly on the thermal efficiency if compared the factor I/Vs and DEP.

The results of the Tab. 3 can be shown better on the Fig. 3, 4, 5 and 6. Figure 3 show the behavior of the thermal efficiency to the processes used (ATIG and TIG), observed that the thermal efficiency in the ATIG process is little compared to the TIG. The average thermal efficiency values are in the range of 66.2% to 68.4% for the processes ATIG and TIG, respectively. The fact of the thermal efficiency was have minor to the ATIG process can be explained in função of the major penetration provide by the active flux. As according Arevalo (2011), when have major penetration have a major heat change with the environment by convection through the reinforcement on the weld root.

Table 2. Results of the thermal efficiency (Nt)

Test	I_m (A)	V_m (V)	$m_i N_2L$ (g)	$m_f N_2L$ (g)	T_a (°C)	E_{sold} (J/mm)	P_{im} (W)	Q_{imp} (J/mm)	Nt (%)
1A	104	10.4	9315.3	9273.5	34.0	432.8	1082	291.23	67
2A	104	11.2	8541.9	8507.2	34.0	464.0	1160	294.05	63
3A	155	11.9	8634.7	8616.8	34.0	408.4	1838	261.14	64
4A	155	12.1	8981.4	8937.8	34.0	416.7	1875	289.20	69
5A	104	11.1	8854.6	8808.9	32.9	461.2	1153	306.94	67
6A	104	11.3	8939.6	8859.2	31.6	468.8	1172	304.65	65
7A	155	11.6	9007.3	8966.6	32.9	398.9	1795	282.16	71
8A	155	12.5	8428.2	8379.6	32.9	429.1	1931	272.78	64
1T	104	9.3	8579.1	8563.6	34.7	388.0	970	262.49	68
2T	104	10.4	8904.5	8867.9	34.7	432.0	1080	286.84	66
3T	155	10.5	9325.8	9288.9	34.8	362.7	1632	267.83	74
4T	155	11.9	9008.0	8959.8	34.8	409.6	1843	285.79	70
5T	104	10.0	8320.3	8277.3	34.7	414.4	1036	295.78	71
6T	104	11.2	9546.5	9529.9	34.8	465.6	1164	245.60	53
7T	155	10.8	8564.5	8529.1	34.6	371.3	1671	266.63	72
8T	155	11.8	8906.9	8852.0	34.7	406.9	1831	298.68	73

I_m : mean current [A]; V_m : mean tension [V]; $m_i N_2L$: initial mass of N_2L more the workpiece on the moment that this it immerse into the dewar [g]; $m_f N_2L$: finale mass of N_2L more the workpiece on the moment wich the loss of N_2L mass be stabilized [g]; T_a : environment temperature in the moment of the weld [°C]; E_{sold} : welding power [J/mm]; P_{im} : instantaneous average power [W]; Q_{imp} : heat input [J/mm].

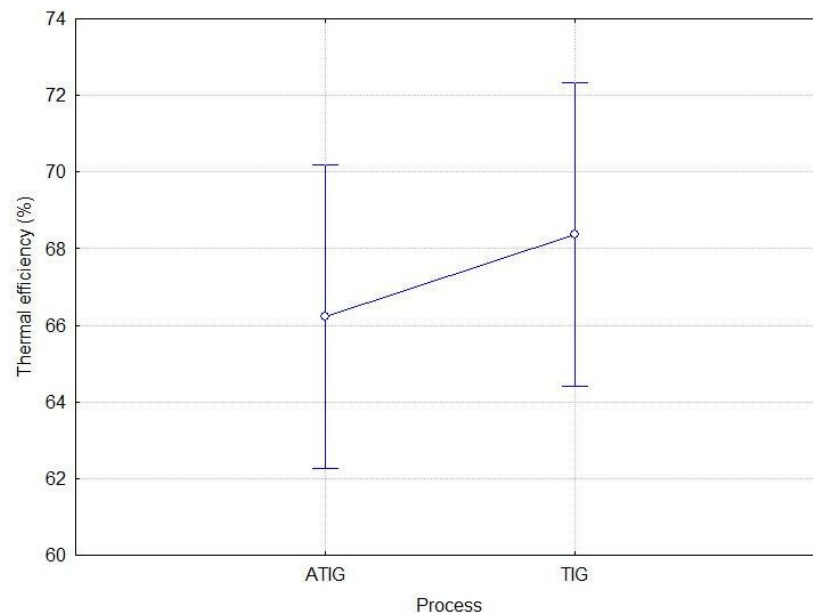


Figure 3. Effect of the TIG and ATIG process on the thermal efficiency.

Thiago José Donegá, Thonson Ferreira Costa, Louriel Oliveira Vilarinho
Thermal Efficiency Measurement During ATIG and TIG Welding

Table 3. ANOVA of thermal efficiency.

Effect	SS	P
Intercept	72477.15	0.000000
Proc	18.41	0.410668
Gas	2.65	0.747527
I/Vs	81.52	0.117657
DEP	54.48	0.183361

Figure 4 presents the tendency of thermal efficiency, comparing the DEP of 2.0 mm and 3.0 mm. Notices that the smaller DEP cause a higher thermal efficiency. This tendency is according the work make by Tsai and Eagar (1985) that compared different distances between electrode and the workpiece in the TIG welding. The authors obtained major heat intensity to the distance of 2.0 mm and this distance increased as the heat intensity decreased. According to Arevalo (2011), the effect of the heat loss, and consequent decrease of thermal efficiency, is amplified by the increase of the arc length. Still according the author, when the DEP is higher, the heat loss on the arc column are higher than the energy produced by the tension increase and, that it is directly influenced by the dimensions of the plasma column. So that, the length increase of the arc results in an increase in the contact area of the plasma column with the environment, generating a larger heat exchange with the environment (Arevalo, 2011).

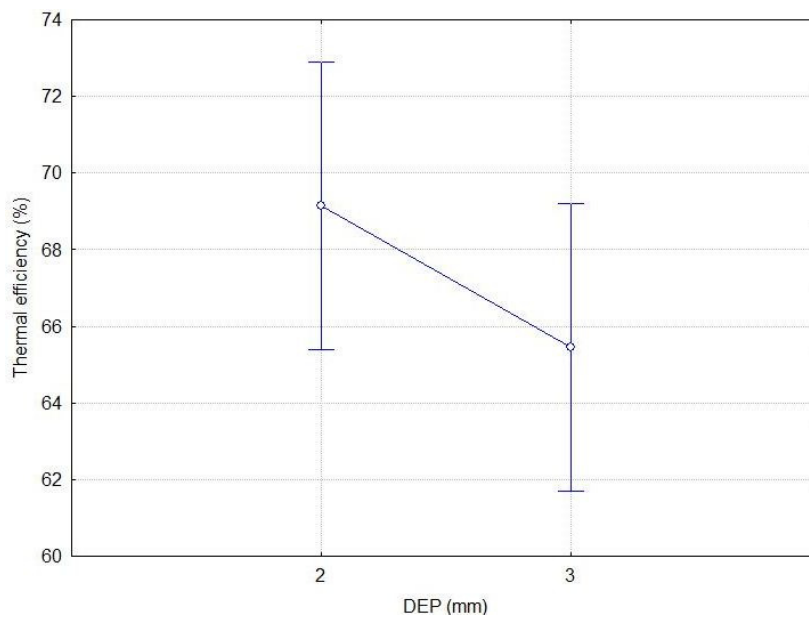


Figure 4. Effect of the DEP on the thermal efficiency.

The Helium own larger thermal conductivity than Argon. Thus, the thermal loss of the arc to environment are higher to gas Helium, wich would to a decrease in a thermal efficiency of the Ar+25%He. On the other hand, the larger thermal conductivity of the Helium deliver greater heat to the workpiece, wich would to a higher thermal efficiency of the Ar+25%He. Some authors (Landim, 2004) found that the arc with Ar and He took a welding with lower thermal efficiency. But other authors (Hiraoka *et al.*, 1998; Cantin and Francis, 2005) mention that this gas mixture leads to higher thermal efficiency. By the result of the ANOVA (Tab. 3), noticed that the gas mixture had no significant effect on thermal efficiency, just by owning these two opposite effects. It is notheworthy that not only the thermal conductivity affected the exchanges thermal between the arc, environment and workpiece, but other physical properties of the gas/plasma, how the specific heat, viscosity, diffusivity, and others.

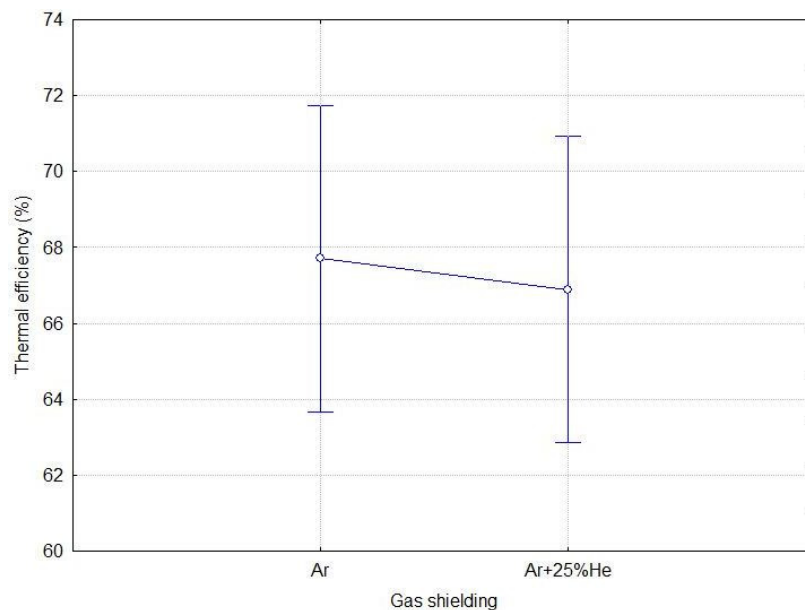


Figure 5. Effect of the gas shielding on the thermal efficiency.

On Figure 6 it can see the effect of I/Vs to the thermal efficiency. On this comparison the thermal efficiency is larger to 6 Amin/cm than 7 Amin/cm. The explanation of this result can be connect with the heat loss by convection. Wich, the means value of penetration to 6 Amin/cm is smaller than 7 Amin/cm (2.799 mm and 3.044 mm respectively). Because, as previously explained, when there is greater penetration there is a greater heat exchange with the environment by convection through the weld root reinforcement. Other factor that can take the value 7 Amin/cm have had a smaller thermal efficiency was the Vs. Because, its speed is lower, making it take longer to be immersed the workpiece in the N_2L , also allowing greater heat exchange with the environment.

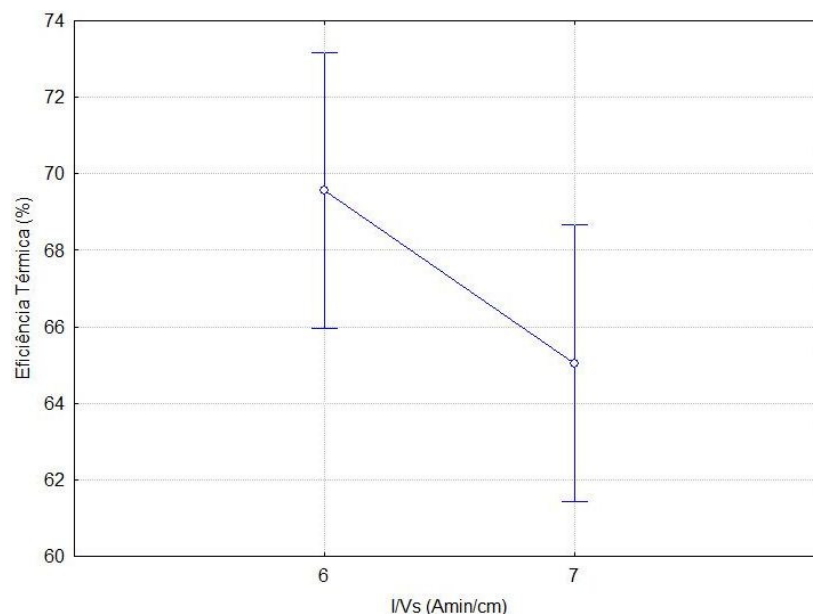


Figure 6. Effect of the I/Vs on the thermal efficiency.

Table 2 shows that the test 6T presented a lower thermal efficiency than other tests, its result in 53%. Such behavior was observed even after repeating the test. In this case, despite to show a high weld power ($E_{solid} = 465.6 \text{ J/mm}$), the conditions used to test 6T, provide a lower heat input ($Q_{imp} = 245.60 \text{ J/mm}$), meaning that the heat duty on the workpiece along the weld by length was very smaller. According to Arevalo (2011), higher heat losses during the welding occur through convection and radiation. These heat losses through radiation generally occur in function of the higher arc column. On this context, a sign to a smaller thermal efficiency of the test 6T can be the increase of the arc column, evidenced through the increase of the bead width, to same conditions of current (100 A) and DEP (3.0 mm), as

can be seen in Tab. 4. Other factor that can have contributed to the heat losses is the higher bead penetration, if compared to the other conventional TIG weld, this test is close to the values achieved by the welding ATIG (Tab. 4). As already stated, the more the penetration bead weld approaches the opposite face of the workpiece, there is greater heat exchange with the environment through convection. Adding to these factors, the lower travel speed provide an increase in losses of heat, both radiation in the arc column and convection in the opposite face of workpiece.

Figure 7 shows the transversal profiles of the bead weld used to the measure of the geometric parameters. It appears that, the samples where applied the active flux, shown an increase on the bead penetration, as well as, a narrowing of the fused zone, analogous to the profile of “goblet”, due the effect of arc constriction.

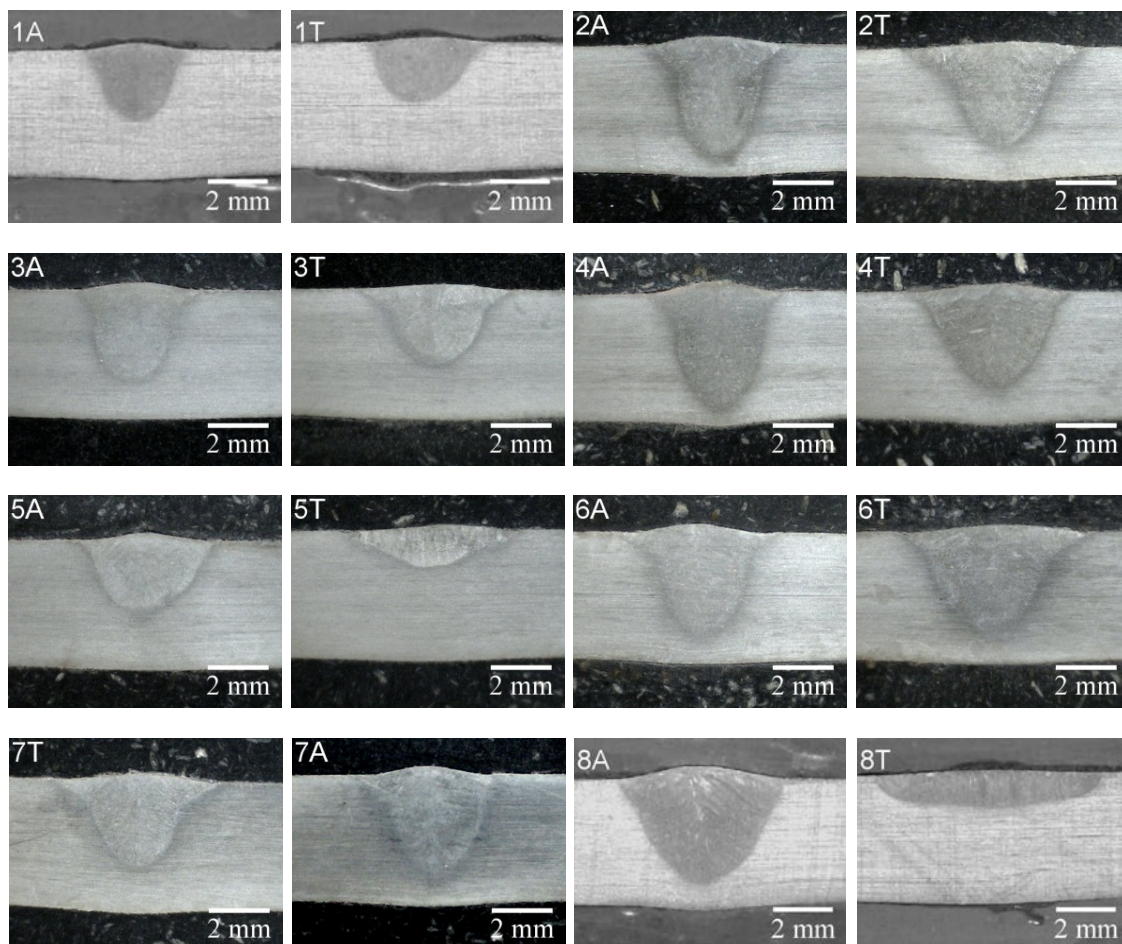


Figure 7. Transversal profiles of the bead weld.

Table 4 shows the results obtained during the measure of the parameters width and penetration, respectively. Observing this table, note that in all cases the average width for the ATIG welds are smaller compared with TIG welds, which is consistent with the literature (Azevedo, 2009), which is characteristic to obtain bead weld closer with application of flux on the TIG weld.

Concerning the penetration, the average values to the ATIG weld were higher compared the TIG weld. Therefore, the penetration of the ATIG weld also is according to the literature (Azevedo, 2009), that obtained results of higher penetration to the weld with flux compared to the weld without flux.

Table 4. Values of width and penetration of the weld beads.

Test	Width (mm)		Penetration (mm)	
	Average	Standard deviation	Average	Standard deviation
1A	3.348	0.002	2.305	0.002
1T	4.128	0.005	1.983	0.002
2A	5.469	0.013	4.015	0.004
2T	6.198	0.003	3.176	0.011
3A	4.010	0.020	2.987	0.008
3T	5.169	0.021	2.603	0.014
4A	4.633	0.002	3.735	0.014
4T	5.653	0.014	3.193	0.047
5A	4.347	0.015	2.365	0.018
5T	5.940	0.006	1.248	0.013
6A	5.321	0.018	3.422	0.021
6T	6.446	0.014	3.238	0.007
7A	4.519	0.007	3.185	0.013
7T	5.587	0.021	2.922	0.012
8A	5.550	0.005	3.463	0.009
8T	7.571	0.004	1.061	0.007

Table 5 presents the significance levels of the welding factors about the geometric parameters of the bead weld, width and penetration. The factors that present significant influence ($p < 0.05$) above the width, were the welding process, the gas shielding and the DEP. In the case of the penetration have nothing significant influence of the factors, but the welding process and the DEP obtained significance levels near the 0.05.

Table 5. Analysis of variance for the parameters width and penetration.

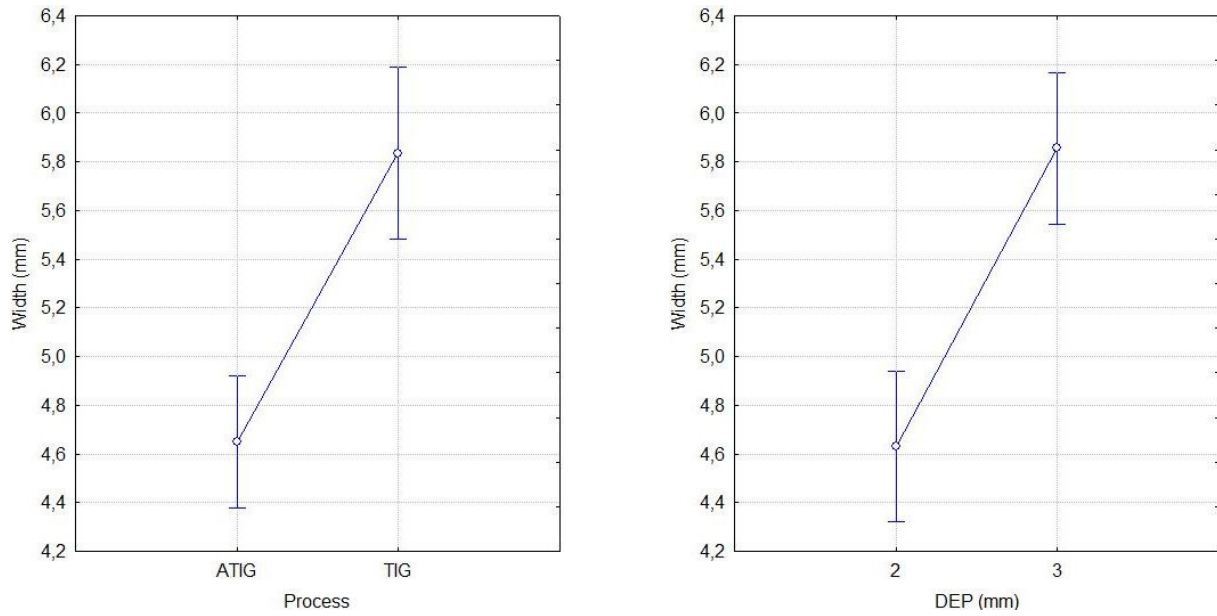
Effect	Width		Penetration	
	SS	P	SS	P
Intercept	43.8353	0.000000	126.0062	0.000010
Processo	5.6347	0.008747	2.2899	0.060359
Gás de proteção	2.7831	0.032632	0.5979	0.271721
I/Vs	0.1397	0.540550	0.1220	0.601048
DEP	5.9939	0.007716	2.0342	0.071734

The effects presents on Table 4 are best visualized in the Fig. 8 and 9, to the width and penetration of the weld beads, respectively. The results are in agreement with what was expected. Figure 8 shows that the average width of the bead weld is larger to the TIG process, to the DEP of 3 mm and, to the gas shielding Ar+25%He. In the case of I/Vs, there is a tendency to get smaller widths for 7 Acm/min. This behavior was expected, because according to what has discussed the ATIG welding process results in an arc constriction and consequently on the narrowing of the bead width. The same way when increases the DEP the bead with also increase (Azevedo, 2011). The mixture Ar+25%He also generate larger bead width, as the addition of He to the Ar cause an increase on the temperature that is caused by the high thermal conductivity of the He, making that more material is melted on the weld surface then results in higher width of the weld beads (Traidia, 2011).

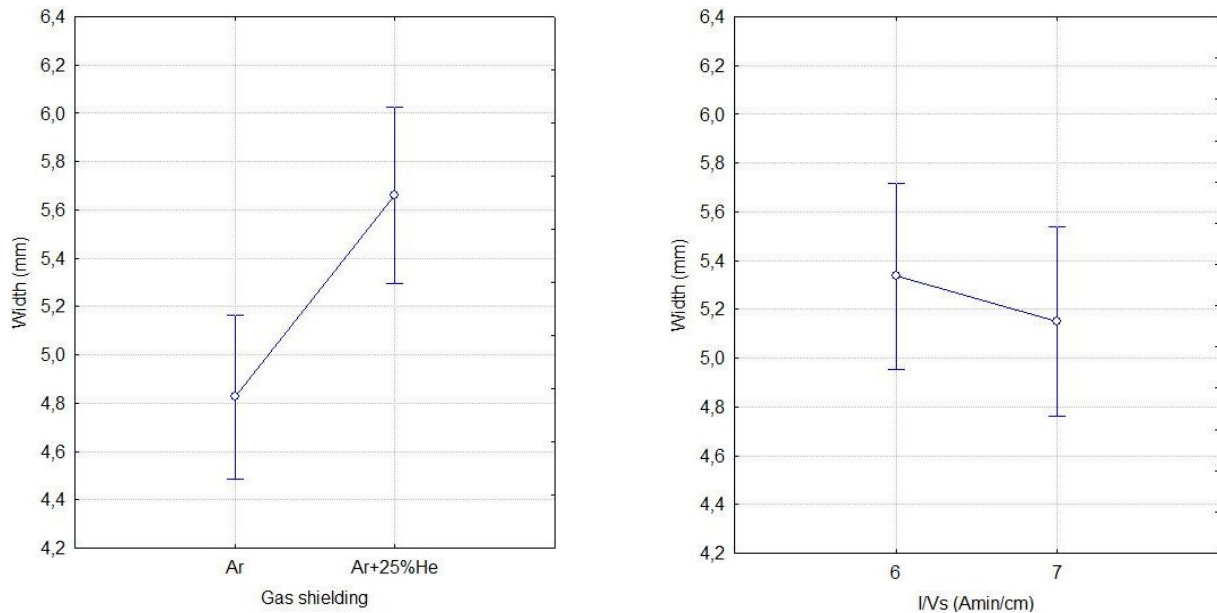
As for the I/Vs 7 Acm/min the tendency to get smaller width may have been due to higher heat loss occurring for this factor. On Figure 9 verifies that on the ATIG process and on the DEP of 3 mm obtained higher penetration. At the same time it is observed that there is a tendency to get less penetration with shielding gas Ar+25%He and the I/Vs of 7 Acm/min. The results are according to the literature. The higher penetration obtained by the ATIG process in comparison to TIG conventional still is a solid process. Already the result obtained by the DEP 3 mm, can happen due the larger arc length obtained by this distance that resulted in a bigger deliver of power by the arc and consequently in a larger penetration of the weld bead. The trend of the gas shielding Ar+25%He result in lower penetration, compared to

Thiago José Donegá, Thonson Ferreira Costa, Louriel Oliveira Vilarinho
 Thermal Efficiency Measurement During ATIG and TIG Welding

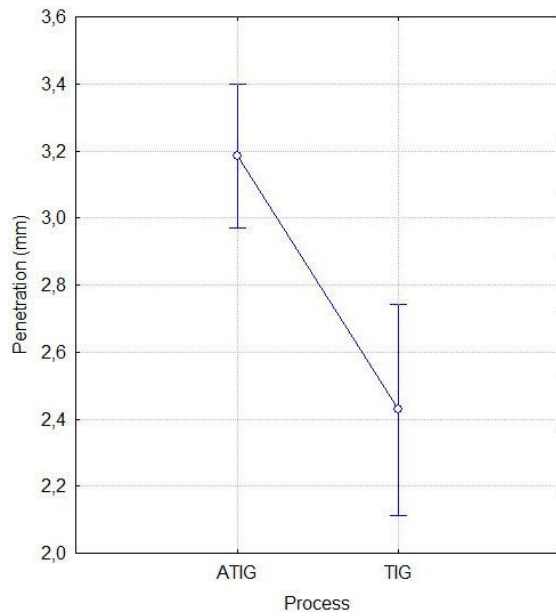
pure Ar, probably due to the tendency of the arc pressure to be lower in atmospheres containing He gas. In the case of I/Vs 7 Acm/min heat losses can be influenced less penetration.



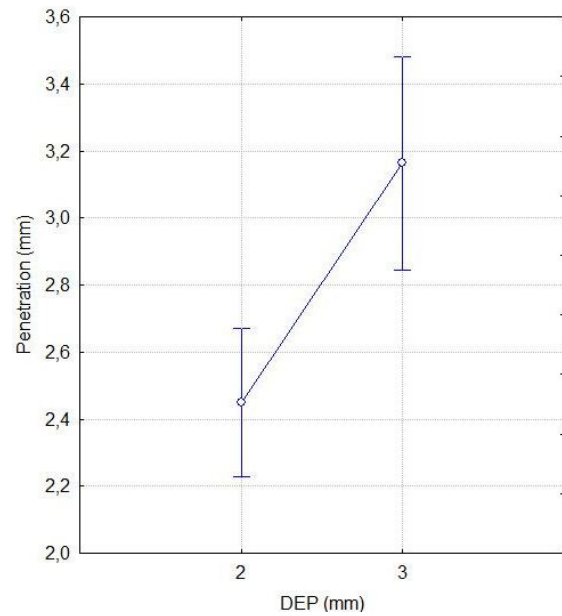
(a) (b)
 Figure 8. Comparison between mean values of width factors: (a) Process (b) DEP



(c) (d)
 Figure 8. Comparison between mean values of width factors: (a) Gas shielding (b) I/Vs

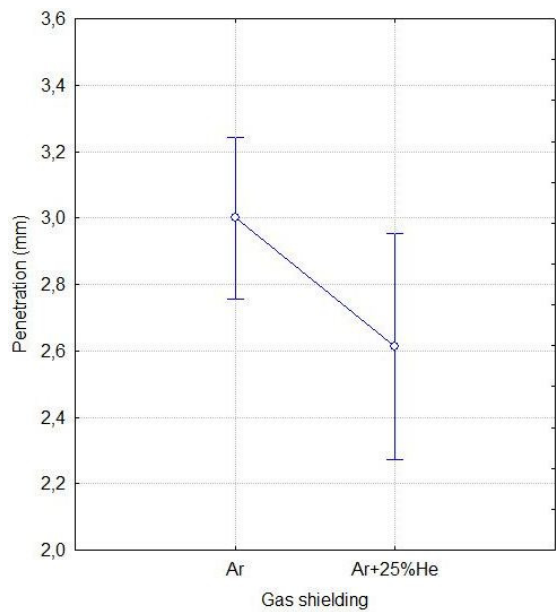


(a)

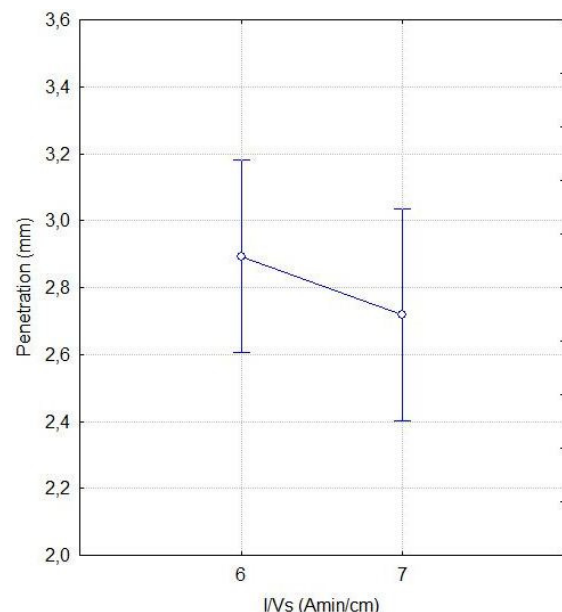


(b)

Figure 9. Comparison between mean values of penetration factors: (a) Process (b) DEP



(c)



(d)

Figure 9. Comparison between mean values of penetration factors: (a) Gas shielding (b) I/Vs

4. CONCLUSIONS

In accordance with previous studies, it is concluded that penetration of the ATIG welding increases and width decreases in comparison with the conventional TIG welding. In addition, it is possible to conclude that the thermal efficiency of the ATIG welding is lower than the efficiency in conventional TIG welding. Thus, there are two main effects, which have different trends. The first is the effect of arc constriction, which tends to increase the current density observed in the smaller bead width. The second effect is the lower thermal efficiency, which leads to a lower heat input, thus reducing penetration. From the results presented, the effect of the arc constriction is more important than the reduction of efficiency.

Thiago José Donegá, Thonson Ferreira Costa, Louriel Oliveira Vilarinho
Thermal Efficiency Measurement During ATIG and TIG Welding

5. ACKNOWLEDGEMENTS

The authors would like to thank FAPEMIG, CNPq and Laprosolda for financial support of this work and participation in the event.

6. REFERENCES

- Anderson, P. C. J. R. and Wiktorowicz, R., 1996. Improving productivity with A-TIG welding. TWI and Air products, USA.
- Arevalo, H. D. H. and Vilarinho, L. O., 2012. Desenvolvimento e Avaliação de Calorímetros por Nitrogênio Líquido e Fluxo Contínuo para Medição de Aporte Térmico. *Soldagem e Inspeção*, São Paulo, Vol. 17, N° 3, p. 236-250, Jul/Set.
- Arevalo, H. D. H., 2011. Desenvolvimento e Avaliação de Calorímetros via Nitrogênio Líquido e Fluxo Contínuo (Água) para Processos de Soldagem. 145 f. Dissertação de Mestrado, Universidade Federal de Uberlândia.
- Azevedo, A. G. L. et al., 2009. Soldagem de um Aço Inoxidável Ferrítico com o Processo A-TIG. *Soldagem e Inspeção*, São Paulo, Vol. 14, N° 1, p. 002-009.
- Cantin, G M.D.; Francis, E J A, 2005. Arc Power and Efficiency in Gas Tungsten Arc Welding of Aluminium. *Science and Technology of welding and joining*10, n. 2: 200-210.
- Dupont, J. N., and Marder, A. R, 1995. Thermal Efficiency of Arc Welding Processes. Department of Material Science and Engineering, 406s-416s.
- Fuershbach, P. K., 1991. A Study of Melting Efficiency in Plasma Arc and Tungsten Arc Welding. *Welding Journal* , 287s-297s.
- Hiraoka, K.; Sakuma, N.; Zijp, E. J, 1998. “Energy Balance in Argon-Helium Mixed Gas Tungsten (TIG) Arcs. Study of Characteristics of Gas Tungsten shielded by Mixed Gases (3rd report).” *Welding International(Welding International)* 12, n. 5: 372-379.
- Howse, D.S., Lucas, W, 2000. Investigation into arc constriction by active fluxes for tungsten inert gas welding. *Sci. Technol. Weld. Join.* 5 (3): 189–193.
- Kumar, V. et al., 2009. “Investigation of the A-TIG Mechanism and the Productivity Benefits in TIG Welding”. In: *JOM-15 - Fifteenth International Conference on the Joining of Materials, Helsingor*. Proceedings of the JOM15 - 03-06/05/2009, p. 1-11.
- Landim, A. S. et al., Comparação entre duas Técnicas Transientes e Tridimensionais para Determinação do Fluxo de Calor em um Processo de Soldagem TIG. In: Congresso Nacional de Engenharia Mecânica - CONEM, 2004, Belém.
- Lucas, W., Howse, D, 1996. Activating flux – increasing the performance and productivity of the TIG and plasma processes. *Weld. Met. Fab.* 64 (1): 11–17.
- Modenesi, P.J.; Apolinario, E.R. and Pereira, I.M, 1999. TIG Welding with Single-Component Fluxes. *Journal of Materials Processing and Technology*, p. 260-265.
- Traidia, A. et al, 2011. Effect of Helium-Argon Mixtures on the Heat Transfer and Fluid Flow in Gas Tungsten Arc Welding. *J. Chem. Chem. Eng.* 5: 854-861.
- Tsai, N. S.; Eagar, T. W, 1985. Distribution of the Heat and Current Fluxes in Gas Tungsten Arcs. *Metallurgical Transactions B*, v. 16B, p. 841-846, December.
- Vilarinho, L. O. et al., 2010a. “Soldagem de Alta Produtividade com o Processo A-TIG para Diferentes Metais de Base”. In: *VI CONEM – Congresso Nacional de Engenharia Mecânica*. Campina Grande/PB, Brazil.
- Vilarinho, L. O. et al., 2010b. “Comparação dos Ciclos Térmicos Obtidos Durante a Soldagem A-TIG e TIG Convencional”. In: *VI CONEM – Congresso Nacional de Engenharia Mecânica*. Campina Grande/PB, Brazil.

7. RESPONSIBILITY NOTICE

The authors are the only responsible for the printed material included in this paper.